BROWN HAREKETİNİN FİZİKSEL SİMÜLASYONU: BASİT DİFÜZYON VE ALT-DİFÜZYON

PHYSICAL SIMULATION of BROWNIAN MOTION: SIMPLE DIFFUSION and SUB-DIFFUSION

Assoc. Prof. Dr. Çağdaş ALLAHVERDİ
ORCID: 0000-0002-6825-5099
Toros University, Faculty of Engineering, Department of Software Engineering,

ÖZET

Fizik bilim dalının önemli temel araştırma konularından biri Brown hareketidir. Robert Brown, 1827 senesinde tek mercekten oluşan bir mikroskop kullanarak sudaki Clarkia pulchella poleninin içini incelemiştir. Bu polenden fışkıran parçacıklar suda gelişigüzel bir biçimde hareket etmektedir. Bu gelişigüzel hareket günümüzde Brown hareketi olarak bilinir. Brown hareketi atom ve molekül dünyasındaki rastgele çarpışmaları gösterir ve bu açıdan bakıldığında aslında atom ve moleküllerin varlığını işaret eder. William Sutherland, Jean Baptiste Perrin, Marian Smoluchowski, Paul Langevin and Albert Einstein'in yaptığı bilimsel çalışmalar sayesinde Brown hareketi anlaşılabilmiştir. Paul Langevin, Newton'un ikinci yasasını kullanarak Brown hareketini tanımlayan diferansiyel denklemi yazmış ve denklemin çözümünü göstermiştir. Langevin denklemi olarak bilinen bu diferansiyel denklem buradaki difüzyon mekanizmasının anlaşılmasını kolaylaştırmaktadır. Langevin eşitliği bu stokastik sistemi anlamamıza yardımcı olur. Bu çalışmada, Brown hareketinin algoritması yazıldı. Algoritmanın yazılım dili olarak Python seçildi. Python programlama dili esnek çalışma yapısı ve çok sayıda işlevsel kütüphaneye sahip olması nedeniyle tercih edildi. Brown hareketinin fiziksel simülasyonunda parçacıklar belirli bir bölge içerisine rastgele bir biçimde dağıtılarak, dağıtılan parçacıklara gelişigüzel çarpışmalar yaptırıldı. Meydana gelen çarpışmalar esnasında momentum ve enerjinin korunumu sağlandı. Ardışık iki çarpışma arasında parçacık süratı sabitken, çarpışmadan sonraki hız, momentum ve enerji korunumu kullanılarak hesaplandı. Simülasyon parametreleri havada hareket eden bir duman parçacığından çıkarılan gerçek fiziksel parametrelere uygun olarak seçildi. Simülasyon, i5 işlemciye sahip sıradan bir bilgisayarda çalıştırıldı. Brown parçacığının diğer parçacığa kütle oranı 10^3-10^5 arasında değiştirildi. Brown parçacığının gelişigüzel yörüngesi gözlemlendi. Brown parçacığının yörüngesi ve hızı kaydedildi. Brown parçacığının ortalama kare yerdeğiştirmesi hesaplandı. Ortalama kare yerdeğiştirmenin zamanla değişimi incelendi. Brown parçacığının hareketinin basit ve alt-difüzyon rejimlerine ait olduğu gösterildi.

Anahtar Kelimeler: Brown Hareketi, Simülasyon, Çarpışmalar, Ortalama Kare Yerdeğiştirme, Difüzyon.

ABSTRACT

Brownian motion is one of the important fundamental research topics in physics. In 1827, Robert Brown examined the inside of Clarkia pulchella pollen in water by using a single-lens microscope. Particles ejected from this pollen move randomly in the water. Nowadays, this random motion is known as Brownian motion. Brownian motion shows random collisions in the world of atoms and molecules, and from this point of view it actually points to the existence of atoms and molecules. Thanks to the scientific works of William Sutherland, Jean Baptiste Perrin, Marian Smoluchowski, Paul Langevin and Albert Einstein, Brownian motion was understood. Paul Langevin wrote the differential equation describing Brownian motion using Newton's second law and showed its solution. This differential equation, known as the Langevin equation, facilitates the understanding of the diffusion mechanism here. The Langevin equation helps us to understand this stochastic system. In this study, the algorithm of Brownian motion was written. Python was chosen as the software language of the algorithm. Python programming language was preferred due to its flexible working structure and having vast number of functional libraries. In the physical simulation of Brownian motion, particles were randomly distributed in a certain region and random collisions were made to the distributed particles. Conservation of momentum and energy was ensured during the collisions. While the particle speed was constant between two successive collisions, the velocity after the collision was calculated using conservation of momentum and energy. The simulation parameters were chosen in accordance with the actual physical parameters extracted from a smoke particle moving in the air. The simulation was run on an ordinary computer with an i5 processor. The mass ratio of the Brownian particle to the other particle was changed between 10^3-10^5. The random trajectory of the Brownian particle was observed. The trajectory and velocity of the Brownian particle were recorded. The mean squared displacement of the Brownian particle was calculated. The variation of the mean squared displacement with time was analyzed. The motion of the Brownian particle was shown to belong to the simple and sub-diffusion regimes.

Keywords: Brownian Motion, Simulation, Collisions, Mean Squared Displacement, Diffusion.

1. Introduction

Robert Brown observed the inside of Clarkia pulchella pollen in water with a single-lens microscope in 1827 (Pearle et al., 2010). The particles ejected from the pollen were moving randomly in the water. The studies of some scientists such as William Sutherland, Albert Einstein, Marian Smoluchowski and Jean Baptiste Perrin clarified this random movement of the particles in water (Bian et al., 2016; Genthon, 2020). This phenomenon is called Brownian motion. It is due to random collision of the particles with water molecules. Today, it is known that random bombardment of a particle with smaller and lighter particles causes random motion of the bombarded particle. Brownian motion can be observed for sufficiently small particles not only in liquid but also in gas media, such as a smoke particle bombarded by air molecules. Paul Langevin formulated Brownian motion by using Newton's second law (Bian et al., 2016; Genthon, 2020; Lemons & Gythiel, 1997).
In this study, Brownian motion has been simulated at two dimensions (2D) via Python. Turtle library has been used for the drawings on the frontend. First, a big and massive particle has been left in a box (that is, a square at 2D) with smaller and identical particles. This big particle is known as Brownian particle. Conservation of momentum and energy has been applied when the particles are collided randomly. Particles are not allowed to go outside the box. The trace of the center of Brownian particle has been tracked during the collisions. The speed and energy of each particle have been calculated constantly. The physical formulas used in the simulation have been explained in the text. The algorithm of Brownian motion has been given.

2. Theory

2.1. Velocities with respect to X'-Y' cartesian coordinate system

The collision of two particles is shown in Figure 1. Conservation of momentum and energy is written as follows if the collision is assumed perfectly elastic. It means that total kinetic energy and total linear momentum are conserved before and after the collision. Conservation of kinetic energy is given in Equation 1. According to X'-Y' cartesian coordinate system, conservation of momentum along the axes is written as in Equation 2 and Equation 3.

$$\frac{1}{2}m_1u_1^2 + \frac{1}{2}m_2u_2^2 = \frac{1}{2}m_1v_1^2 + \frac{1}{2}m_2v_2^2 \tag{1}$$

$$m_1 u_{1X'} + m_2 u_{2X'} = m_1 v_{1X'} + m_2 v_{2X'} \quad (2)$$
$$m_1 u_{1Y'} + m_2 u_{2Y'} = m_1 v_{1Y'} + m_2 v_{2Y'} \quad (3)$$

where $m_1, m_2, u_1, u_2, v_1, v_2$ are mass of particle 1, mass of particle 2, speed of particle 1 before the collision, speed of particle 2 before the collision, speed of particle 1 after the collision, speed of particle 2 after the collision, respectively. $u_{1X'}, u_{2X'}, v_{1X'}, v_{2X'}$ are velocity of particle 1 along X' before the collision, velocity of particle 2 along X' before the collision, velocity of particle 1 along X' after the collision, and velocity of particle 2 along X' after the collision. Similarly, $u_{1Y'}, u_{2Y'}, v_{1Y'}, v_{2Y'}$ are velocity of particle 1 along Y' before the collision, velocity of particle 2 along Y' before the collision, velocity of particle 1 along Y' after the collision, and velocity of particle 2 along Y' after the collision, respectively (See Figure 2). Here, $u_1^2, u_2^2, v_1^2, v_2^2$ are written as follows.

$$u_1^2 = u_{1X'}^2 + u_{1Y'}^2 \quad (4)$$
$$u_2^2 = u_{2X'}^2 + u_{2Y'}^2 \quad (5)$$
$$v_1^2 = v_{1X'}^2 + v_{1Y'}^2 \quad (6)$$
$$v_2^2 = v_{2X'}^2 + v_{2Y'}^2 \quad (7)$$

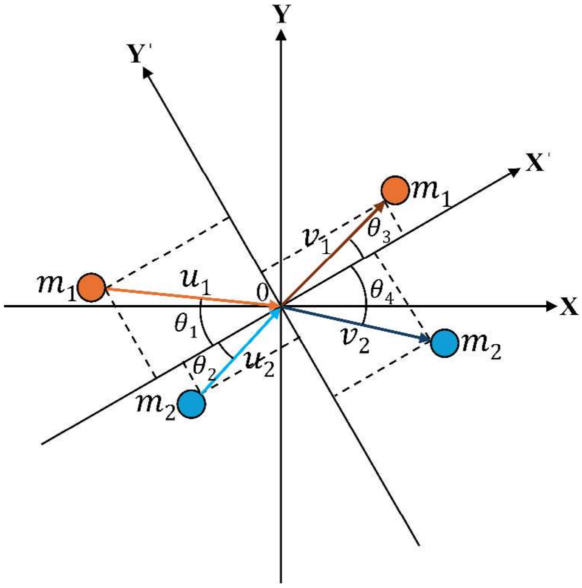

Figure 1. Collision of two particles. m_1 and m_2 are masses of the particles shown with orange and blue colors. u_1 and u_2 are velocities of the particles before the collision, and v_1 and v_2 are velocities of the particles after the collision. θ_1, θ_2, θ_3 and θ_4 are angles between velocity vectors ($\vec{u}_1$, $\vec{u}_2$, $\vec{v}_1$ and $\vec{v}_2$) and X' axis.

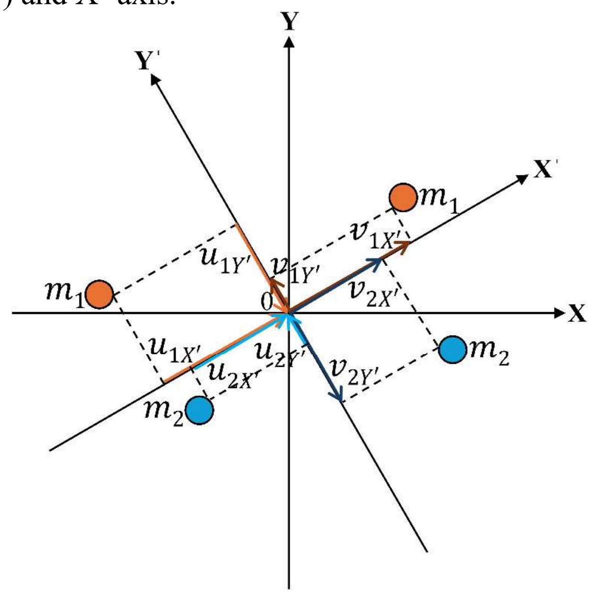

Figure 2. Components of velocity vectors before and after the collision.

Along the X' axis, Equations 8 and 9 can be written. Momentum or velocity of particle along the X' axis before and after the collision is same.

$$m_1 u_{1X'} = m_1 v_{1X'} \quad (8)$$

$$m_2 u_{2X'} = m_2 v_{2X'} \quad (9)$$

$$u_{1X'} = v_{1X'} \quad (10)$$

$$u_{2X'} = v_{2X'} \quad (11)$$

Equations 4-7 are substituted in Equation 1 and then Equations 10 and 11 are used. Thus, Equation 12 is obtained.

$$m_1 u_{1Y'}^2 + m_2 u_{2Y'}^2 = m_1 v_{1Y'}^2 + m_2 v_{2Y'}^2 \quad (12)$$

Here, it is needed other description which is called coefficient of restitution (e). The coefficient of restitution is velocity difference of two particles after the collision along Y' axis divided by velocity difference of these two particles before the collision along Y' axis.

$$e = -\frac{v_{1Y'} - v_{2Y'}}{u_{1Y'} - u_{2Y'}} \quad (13)$$

e is taken 1 for perfectly elastic collision. Thus, Equation 14 is obtained.

$$u_{1Y'} + v_{1Y'} = v_{2Y'} + u_{2Y'} \quad (14)$$

Equation 12 can be written as follows.

$$m_1\left(u_{1Y'}^2 - v_{1Y'}^2\right) = m_2\left(v_{2Y'}^2 - u_{2Y'}^2\right) \quad (15)$$

$$m_1(u_{1Y'} - v_{1Y'})(u_{1Y'} + v_{1Y'}) = m_2(v_{2Y'} - u_{2Y'})(v_{2Y'} + u_{2Y'}) \quad (16)$$

If Equation 14 is substituted in Equation 16, Equation 17 is attained.

$$m_1(u_{1Y'} - v_{1Y'}) = m_2(v_{2Y'} - u_{2Y'}) \quad (17)$$

Finally, by using Equations 14 and 17, the Y'-components of the velocities of the particles after the collision are derived depending on those before the collision as follows.

$$v_{1Y'} = \frac{(m_1 - m_2)u_{1Y'} + 2m_2 u_{2Y'}}{m_1 + m_2} \quad (18)$$

$$v_{2Y'} = \frac{(m_2 - m_1)u_{2Y'} + 2m_1 u_{1Y'}}{m_1 + m_2} \quad (19)$$

Thus, the speeds of two particles after the collision are calculated as below.

$$v_1 = \sqrt{v_{1X'}^2 + v_{1Y'}^2} = \sqrt{u_{1X'}^2 + \left(\frac{(m_1 - m_2)u_{1Y'} + 2m_2 u_{2Y'}}{m_1 + m_2}\right)^2} \quad (20)$$

$$v_2 = \sqrt{v_{2X'}^2 + v_{2Y'}^2} = \sqrt{u_{2X'}^2 + \left(\frac{(m_2 - m_1)u_{2Y'} + 2m_1 u_{1Y'}}{m_1 + m_2}\right)^2} \quad (21)$$

The acute angles between these velocities (v_1 and v_2) and the X' axis after the collision are found as follows (See Figures 1 and 2).

$$\theta_3 = tan^{-1}\left(\left|\frac{v_{1Y'}}{v_{1X'}}\right|\right) \quad (22)$$

$$\theta_4 = tan^{-1}\left(\left|\frac{v_{2Y'}}{v_{2X'}}\right|\right) \quad (23)$$

As understood from Equations 22 and 23, in X'-Y' coordinate system, β which is the scattering angle of a particle after the collision can be written as follows.

$$\beta = tan^{-1}\left(\left|\frac{v_{nY'}}{v_{nX'}}\right|\right) \quad (24)$$

Here, n is particle number (1 or 2). It is important to note that β is positive and in the range of $\left[0, \frac{\pi}{2}\right]$. The quadrant of β is found by looking the signs of $v_{nX'}$ and $v_{nY'}$. Table 1 explains this situation. In Table 1, β_T refers to the angle in counterclockwise direction from X' axis to velocity vector of scattering particle (See Figure 3).

Table 1. The quadrant of β for X'-Y' coordinate system. Transition from β to β_T is given.

$\beta \rightarrow \beta_T$	Sign of $v_{nY'}$ Positive (+)	Sign of $v_{nY'}$ Negative (-)

Sign of $v_{nX'}$ Positive (+)	β is at quadrant I $\beta_T = \beta$	β is at quadrant IV $\beta_T = 2\pi - \beta$
Sign of $v_{nX'}$ Negative (-)	β is at quadrant II $\beta_T = \pi - \beta$	β is at quadrant III $\beta_T = \pi + \beta$

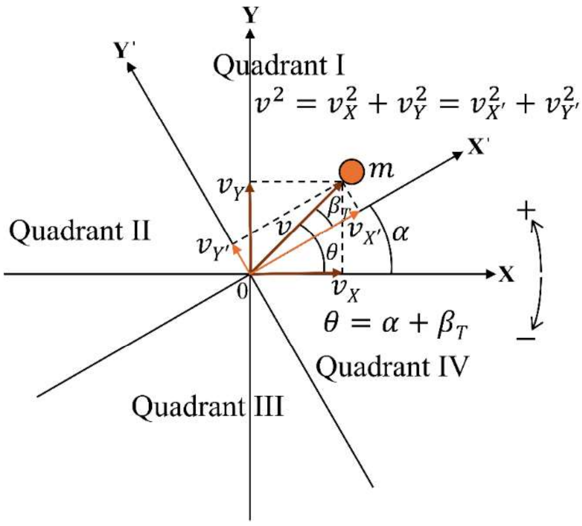

Figure 3. Quadrants of X'-Y' coordinate system. v_X and v_Y are components of velocity vector v at X-Y cartesian coordinate system. $v_{X'}$ and $v_{Y'}$ are components of velocity vector v at X'-Y' cartesian coordinate system. β_T is the counterclockwise angle from the X'-axis to the velocity vector v of the colliding particle. α is the clockwise or counterclockwise rotation angle of X' axis with respect to X axis. θ is the angle between the velocity vector v and X axis. Clockwise and counterclockwise angles are negative (-) and positive (+), respectively.

2.2.Rotation Angle Between X and X' axes

As seen from Figure 4, rotation angle between X and X' axes is α. X' axis is tangential to both particle 1 and particle 2. However, Y' axis passes through the centers of the particles and perpendicular to X' axis. α can be calculated as follows. First, slope of Y' ($m_{Y'}$) is calculated and then, in turn, slope of X' ($m_{X'}$) and α is found in the reference system of X-Y.

$$m_{Y'} = \frac{Y_2 - Y_1}{X_2 - X_1} \tag{25}$$

$$m_{X'} = -\frac{1}{m_{Y'}} \tag{26}$$

$$\alpha = tan^{-1}(m_{X'}) \tag{27}$$

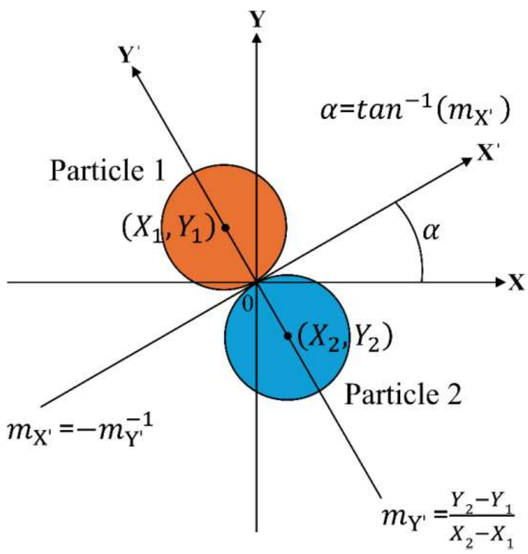

Figure 4. Rotation angle (α) between X and X' axes. (X_1, Y_1) and (X_2, Y_2) are center coordinates of two particles. $m_{X'}$ and $m_{Y'}$ are slopes of the X' and Y' axes.

2.3.Velocities with respect to X-Y cartesian coordinate system

As seen from Figure 3, θ is found after calculation of α and β_T. If it exceeds 2π (360^o), 2π is subtracted from θ. If it is negative, it means that it deviates in the clockwise direction from the X axis.

$$\theta = \alpha + \beta_T \tag{28}$$

X and Y components of velocity vector of each particle after the collision are calculated as follows.

$$v_X = v.cos\theta = v.cos(\alpha + \beta_T) \tag{29}$$

$$v_Y = v.sin\theta = v.sin(\alpha + \beta_T) \tag{30}$$

Thus, X and Y components of v_1 and v_2 (Velocities of particles after the collision. See Figure 1) are given as follows.

$$v_{1X} = v_1.cos(\alpha + \beta_{T1}) \tag{31}$$

$$v_{1Y} = v_1.sin(\alpha + \beta_{T1}) \tag{32}$$

$$v_{2X} = v_2.cos(\alpha + \beta_{T2}) \tag{33}$$

$$v_{2Y} = v_2.sin(\alpha + \beta_{T2}) \tag{34}$$

α will be same for two collided particles. However, β_T is different for particle 1 and particle 2. β_{T1} is β_T for particle 1 and β_{T2} is β_T for particle 2.

2.4.Collision of Particle with Wall

Particles are placed in a restricted area. Here, this area is a square and called box in this text. Particles cannot pass through the walls of this box. They are reflected from the walls when they hit the walls. Such a reflection (bouncing) is shown in Figure 5. The particle hits the wall and returns backward. The particle would be at point B in the next step if it had passed the wall. The particle is reflected to point C so that it remains inside the box. C point is reflection of B point. Thus, the distance taken by the particle from A to C is same as the distance from A to B. The relations are given as follows.

$$|AP| + |PC| = |AP| + |PB| \tag{35}$$

$$|PC| = |PB| \tag{36}$$

$$|CS| = |BS| \tag{37}$$

Similar reflection operations can be shown for the other walls. As seen from Figure 5, the boundary of the particle cannot pass the lines of the box. For this right wall, it is written as follows.

$$X_1 + R \leq \frac{W}{2}\ (For\ the\ right\ wall\ of\ the\ box) \tag{38}$$

where X_1 is the X coordinate of center of the particle, R is the radius of the particle, and W is the wide of the box. Similar equations are written for the other walls. These are:

$$X_1 - R \geq -\frac{W}{2} (Left\ wall) \tag{39}$$

$$Y_1 + R \leq \frac{W}{2}\ (Upper\ wall) \tag{40}$$

$$Y_1 - R \geq -\frac{W}{2}\ (Lower\ wall) \tag{41}$$

If any of these equations (Equations 38-41) is not satisfied, the particle is reflected from the wall. The box can be assumed to be a rectangle. In this case, W will be W_1 (wide) for Equations 38 and 39 and W_2 (height) for Equations 40 and 41.

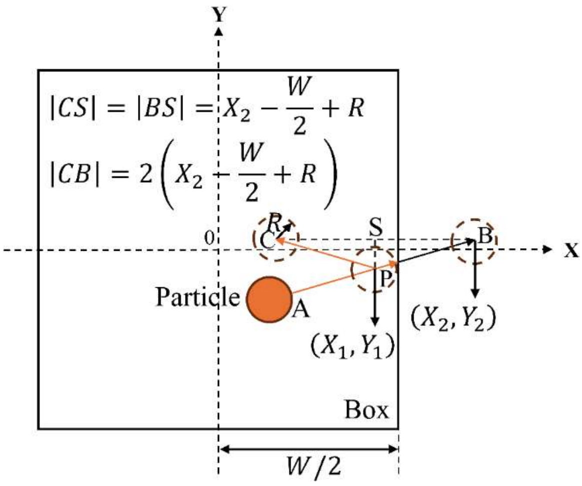

Figure 5. Bouncing off a particle from the wall of the box. W is the wide of the box. R is the radius of the particle. Particle A tracks APC pathway. X_1 and Y_1 are center coordinate of the particle. Point C is the reflection of point B with respect to vertical line SP.

2.5.Collision of Particle with Another Particle

If the distance between the centers of any two particles are smaller than the sum of their radii, these particles are accepted as collided. Thus, there is a collision between these two particles. This situation is stated as follows.

$$\sqrt{(X_1 - X_2)^2 + (Y_1 - Y_2)^2} \leq R_1 + R_2 \tag{42}$$

$$(X_1 - X_2)^2 + (Y_1 - Y_2)^2 \leq (R_1 + R_2)^2 \tag{43}$$

where X_1 and Y_1 are coordinates of center of particle 1, X_2 and Y_2 are coordinates of center of particle 2, and R_1 and R_2 are radii of particle 1 and 2, respectively (See Figure 6).

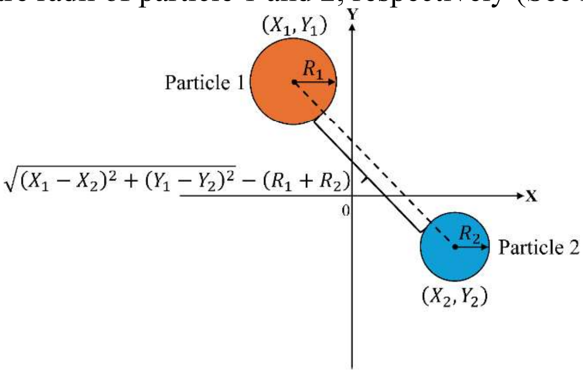

Figure 6. The distance between two particles.

2.6.Mean Free Path of Particles

In the box, each particle makes random consecutive collisions. These are particle-particle or particle-wall collisions. The average of the distances traveled by any particle in successive collisions gives its mean free path. The mean free path of the particle is described as in Equation 44.

$$\lambda = \frac{\sum_{i=1}^{n} l_i}{n} \tag{44}$$

where λ is the mean free path, l_i is the distance between two consecutive collisions and n is the number of these distances (See Figure 7). The mean free path for gas molecules is given as follows.

$$\lambda = \frac{k_B T}{\sqrt{2}\pi D^2 P} \tag{45}$$

Here, k_B is Boltzmann constant, T is temperature, D is kinetic diameter of gas molecule and P is pressure.

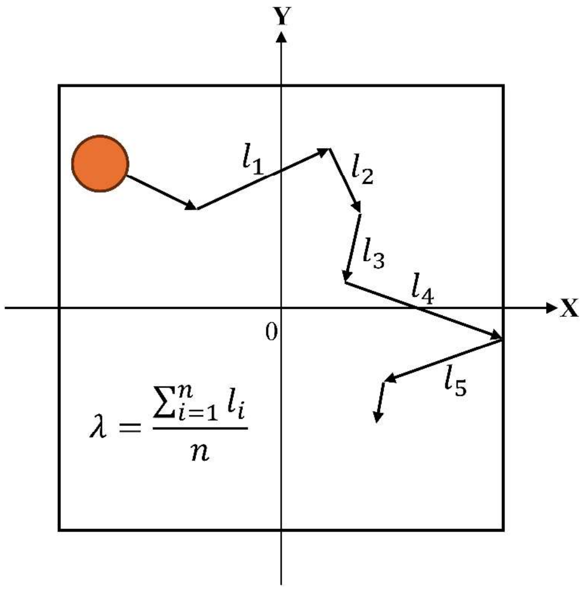

Figure 7. Mean free path of a particle. λ is mean free path and l_i is the distance between two successive collisions.

3. Algorithm of Brownian motion

The algorithm of Brownian motion is shown in Figure 8. Particle number N is entered into the program. N is the number of all particles in the box. The Brownian particle is placed at the center of the box. It is at rest. Other small identical particles are randomly distributed around the Brownian particle in the box. Velocities are randomly given to the small particles (At the beginning, their speeds are the same). They start to move in the box with time. Their displacements are calculated by the formula of velocity×time interval ($\Delta x = v\Delta t$). If particles collide with any wall of the box or collide with each other, they are bounced off according to the laws of conservation of momentum and energy. The trajectory of the Brownian particle is monitored during these collisions. If the Brownian particle hits the wall, the program stops running.

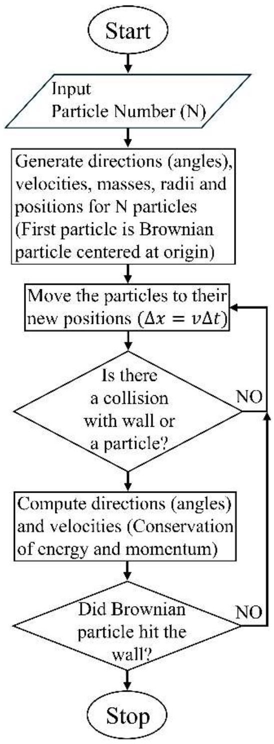

Figure 8. Flowchart of the Brownian motion.

4. Results and Discussion

In this study, Brownian motion of a particle in air (like a small cigarette smoke particle) was visualized. As a simplification, the air in the box was assumed to consist entirely of nitrogen (N_2) molecules. First, some basic physical parameters of this system were taken from the literature (Chen et al., 1990), then some parameters were calculated by using the physical equations. These parameters are listed in Table 1. The calculations are based on standard conditions for temperature and pressure (273.15 K and 10^5 Pa).

Table 1. Physical properties of smoke and N_2 particles.

Physical Properties	Smoke particle (Brownian particle)	N_2 molecule (Particles)
Density	1.12 g/cm^3*	1.2506 g/L
Diameter	0.22 μm*	364 pm
Mass	6.24×10^{-18} kg	4.65×10^{-26} kg
Velocity	0 (Initially)	493.15 m/s
Mean Free Path	-	6.40×10^{-8} m

*From reference (Chen et al., 1990).

A conversion factor from meter to pixel was formed to be able to demonstrate this system at the computer screen. The number of particles in the box, their velocities and sizes, the size of the box were adjusted according to the values in Table 1. In these simulations, a mean free path close to the value given in Table 1 was generated for N_2 particles in the box, excluding Brownian particle. It is assumed that there is no acceleration of the particles between collisions. In fact, the ratio of mass of smoke particle to mass of N_2 particles is around 10^8. However, in our demonstrations, the mass ratio of a smoke particle to N_2 was changed from 10^3 to 10^5 to produce faster results in an ordinary laptop nowadays. The processor of the laptop used in the simulations was Intel® Core™ i5-8265U.

The results are shown in Figures 9 and 10. In our simulations, 0.22 μm (the diameter of Brownian particle) corresponds to 362 pixels. The width and height of the box are 450 pixels. In Figure 9, the mass ratio of the Brownian particle to small particle is 10^3 ($m_B/m=10^3$). The total number of particles in the box is 14 particles (N=14 particles) so that the mean free path of the particles in the box (except the Brownian particle) has been kept almost constant (around 105.3 px). Running time of the program (t), number of collisions of the Brownian particle (NCB) with other particles and total distance traveled by the Brownian particle (TDB) have been measured. The text in each figure indicates these experimental parameters.

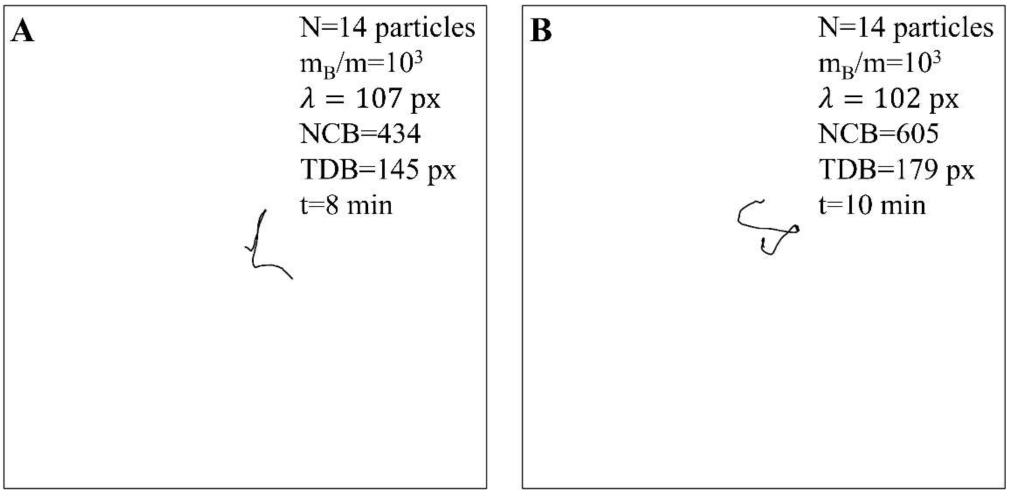

Figure 9. Random trajectory of Brownian particle. For Figures 9A and 9B, square shows the box. Solid curve in the box indicates random trajectory of the Brownian particle. Experimental

parameters are given at the top right of the box. N is the number of all particles in the box. m_B/m is the ratio of mass of Brownian particle to that of small particle. λ is the mean free path of the small particles. NCB is the number of collisions of the Brownian particle with small particles. TDB is total distance traveled by the Brownian particle. Running time of the program is shown with t.

In Figure 10, six simulations of Brownian motion are given. The mass ratio of the Brownian particle to small particle is 10^4 for Figures 10A, 10B and 10C and 10^5 for Figures 10D, 10E and 10F. The random motion of the Brownian particle has been shown in all these figures. The motion given in Figure 10F is plotted on X-Y plane in Figure 11. As seen in Figure 12, the normalized speed of the Brownian particle is added as a third dimension for Figure 11. The speed of the Brownian particle increases and decreases randomly. However, it takes lowest values for the turning points of the particle as expected. Such a point is seen at the coordinate of (18, -17) in Figure 11.

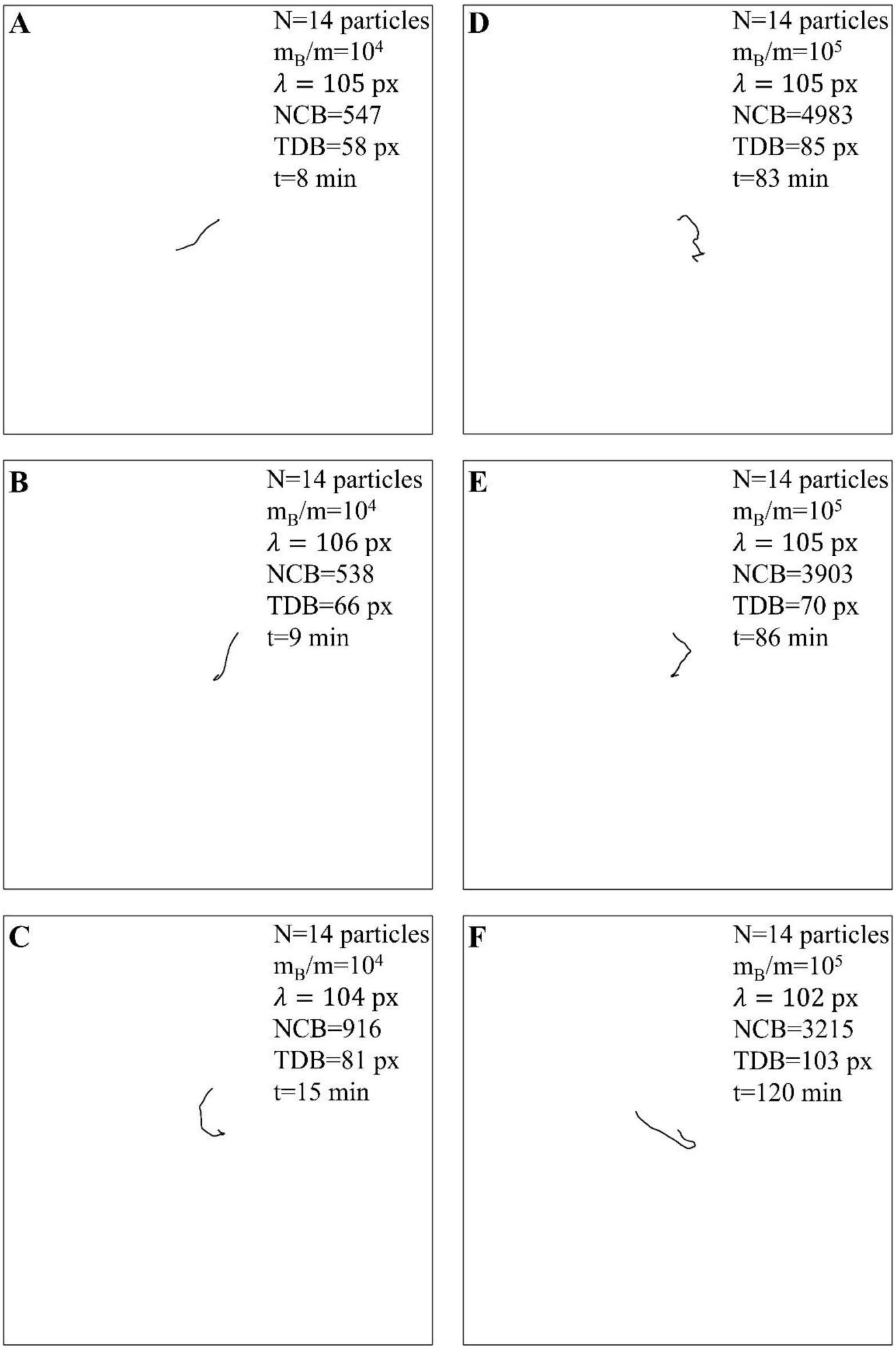

Figure 10. Random trajectory of Brownian particle. Six experimental studies from 10A to 10F are shown. Experimental parameters are given at the top right of the box.

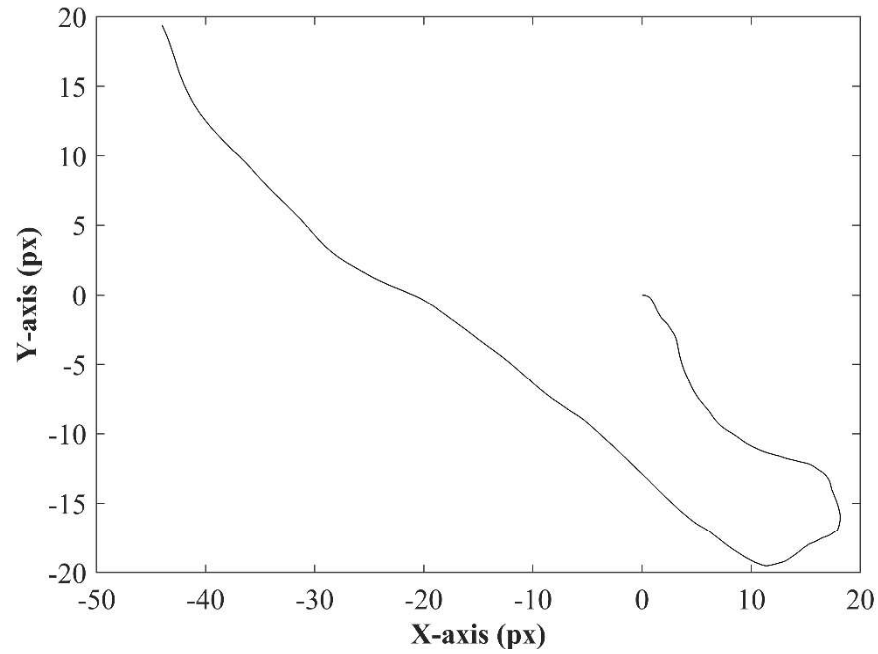

Figure 11. Random trajectory of Brownian particle on X-Y coordinate plane (See Figure 10F). Experimental parameters are given at Figure 10F. Units of X and Y are in pixels. (0,0) is the beginning point of Brownian motion.

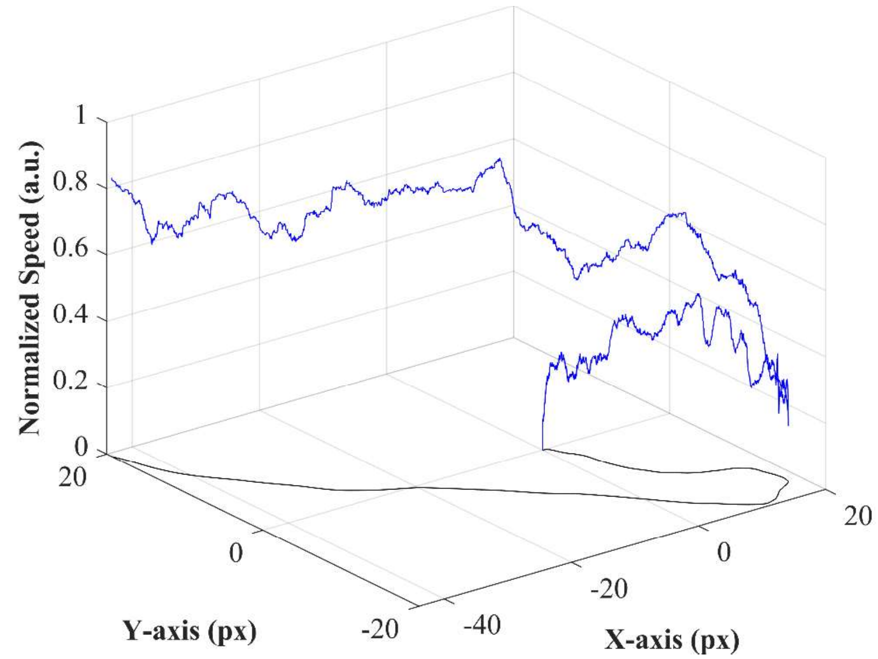

Figure 12. Speed of Brownian particle. Black curve shows position (X, Y) of the Brownian particle (See Figures 10F and 11). Blue curve indicates its normalized speed in arbitrary unit (a.u.). (0,0) is the beginning point of Brownian motion.

In Figure 13, two random trajectories of the Brownian particle are shown. These trajectories have been obtained for N=14 particles and $m_B/m=10^5$. When the Brownian particle followed path 1, it collided randomly with other particles 2275 times (NCB=2275). The number of these collisions is 3486 for path 2. Mean squared displacements (MSDs) have been computed from their trajectories (Wang et al., 2014; Miné-Hattab & Chiolo, 2020). The MSDs are shown in Figure 14. As seen from the figure, the MSD increases linearly with time after ~800 for curve 1 (MSD α t). It shows that the motion seen on path 1 is a simple diffusion. However, there is a plateau for curve 2. It is important to emphasize that the Brownian particle moves clockwise by means of many particle collisions like a particle confined in a box when it follows path 2. It indicates sub-diffusion due to partially confined motion.

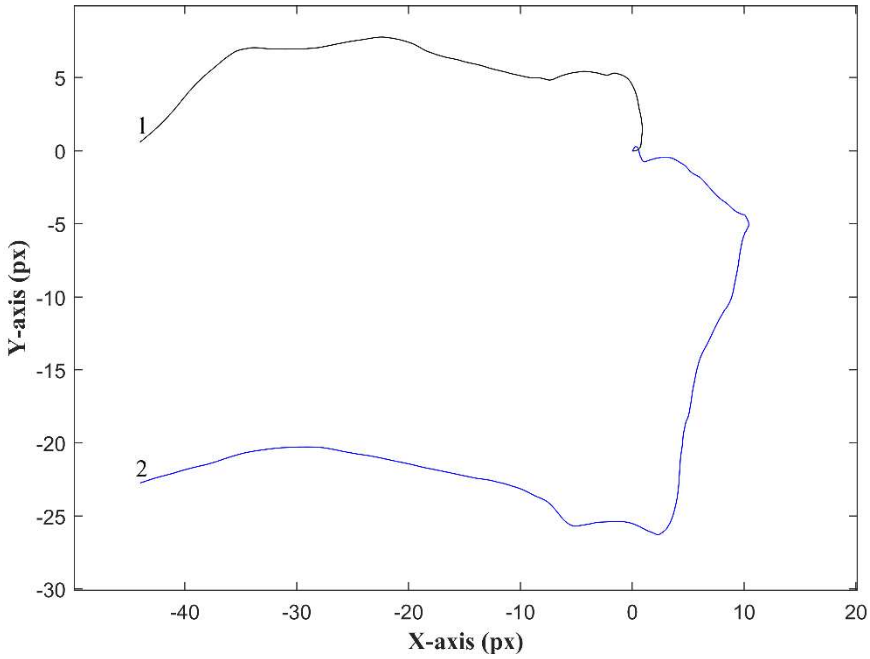

Figure 13. Two different random trajectories of the Brownian particle. Path 1 (black curve) and path 2 (blue curve) are produced for N=14 particles and $m_B/m=10^5$ mass ratio.

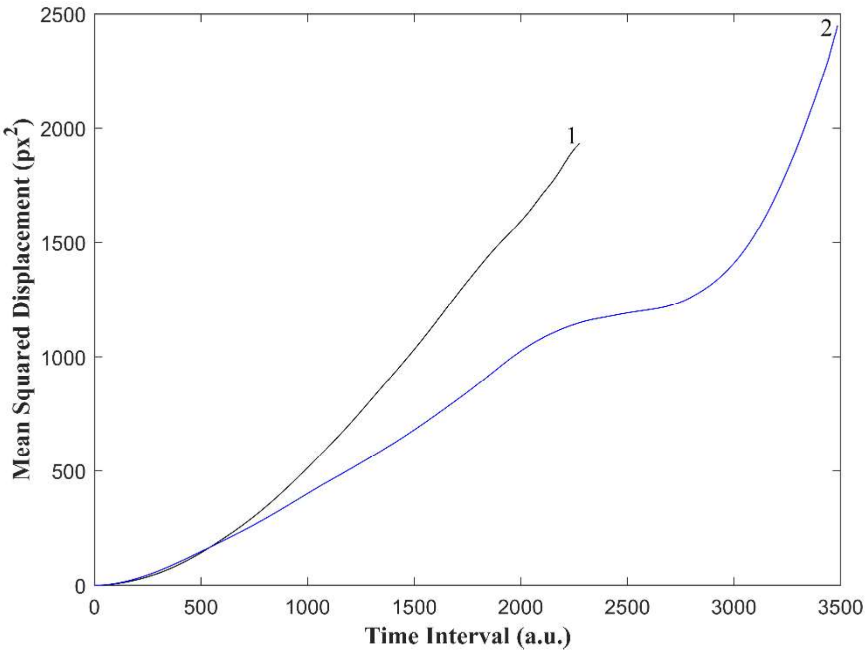

Figure 14. Mean squared displacement versus time interval. 1) for path 1 in Figure 13 and 2) for path 2 in Figure 13. The time interval corresponds to the difference between the sequence numbers of collision points on the trajectory (See Reference (Wang et al., 2014) for the computation).

Different successful approaches for the simulation of Brownian motion are seen in the literature (Snyder, 2023; Liu & Jia, 2021). This study presents a clearer, simpler and more fundamental version of Brownian motion.

5. Conclusion

In this work, simulation of Brownian motion has been studied. The algorithm of the Brownian motion has been written via Python. Laws of conservation of momentum and energy have been applied to the colliding particles in a box. Mean free path of the particles (except Brownian particle) has been kept constant in the simulations. The mass of the Brownian particle has been increased to 10^5 times the mass of other particles. The Brownian motion has been demonstrated in minutes by a common laptop having Intel® Core™ i5 processor. Above the mass ratio of 10^5, the simulation time needed has sharply increased. All collisions and speeds have been recorded during the simulation. Random trajectory of Brownian particle has been shown. The character of the diffusion has been determined by computing the mean squared displacement.

References

Bian, X., Kim, C., & Karniadakis, G.E. (2016). 111 years of Brownian motion, *Soft Matter*, *12*(30), 6331-6346. https://doi.org/10.1039/C6SM01153E

Chen, B. T., Namenyi, J., Yeh, H. C., Mauderly, J. L., & Cuddihy, R. G. (1990). Physical Characterization of Cigarette Smoke Aerosol Generated from a Walton Smoke Machine. *Aerosol Science and Technology*, *12*(2), 364-375. https://doi.org/10.1080/02786829008959352

Genthon, A. (2020). The concept of velocity in the history of Brownian motion, *Eur. Phys. J. H*, *45*, 49-105. https://doi.org/10.1140/epjh/e2020-10009-8

Lemons, D. S., & Gythiel, A. (1997). Paul Langevin's 1908 paper "On the Theory of Brownian Motion". *Am. J. Phys.*, *65*(11), 1079-1081. https://doi.org/10.1119/1.18725

Liu, Z., & Jia, Y. (2021, July). Two Simulation Methods of Brownian Motion. *Journal of Physics: Conference Series*, *2012*(2021), 012015. https://doi.org/10.1088/1742-6596/2012/1/012015

Miné-Hattab, J., & Chiolo, I. (2020). Complex Chromatin Motions for DNA Repair. *Front. Genet.*, *11*(800), 1-16. https://doi.org/10.3389/fgene.2020.00800

Pearle, P., Collett, B., Bart, K., Bilderback, D., Newman, D., & Samuels, S. (2010). What Brown saw and you can too. *Am. J. Phys.*, *78*(12), 1278-1289. https://doi.org/10.1119/1.3475685

Snyder, B. (2023). *Using the Langevin Equation to Verify a Single-Particle Brownian Motion Simulation*[Undergraduate thesis, Oregon State University]. ScholarsArchive@OSU. https://ir.library.oregonstate.edu/concern/undergraduate_thesis_or_projects/hm50v085w

Wang, Y., Jeong, Y., Jhiang, S. M., Yu, L., & Menq, C.-H. (2014). Quantitative Characterization of Cell Behaviors through Cell Cycle Progression via Automated Cell Tracking. *Plos One*, *9*(6), e98762. https://doi.org/10.1371/journal.pone.0098762

ÇUKUROVA
14TH INTERNATIONAL SCIENTIFIC RESEARCHES CONFERENCE

March 24-26, 2025

ADANA

PROCEEDINGS BOOK

EDITORS

Dr. Ethem İlhan ŞAHİN

Dr. Jamal Eldin Fadoul Mohammed IBRAHIM

ISBN: 979-8-89695-056-1

ÇUKUROVA 14th INTERNATIONAL SCIENTIFIC RESEARCHES CONFERENCE

March 24-26, 2025
Adana / TURKIYE

PROCEEDINGS BOOK

EDITORS

Dr. Ethem İlhan ŞAHİN
Dr. Jamal Eldin Fadoul Mohammed IBRAHIM

Issued: 17.04.2025

ISBN: 979-8-89695-056-1

ÇUKUROVA 14TH INTERNATIONAL SCIENTIFIC RESEARCHES CONFERENCE

March 24-26, 2025
Adana, Türkiye

PROCEEDING BOOK

Dr. Ethem İlhan ŞAHİN
Dr. Jamal Eldin Fadoul Mohammed IBRAHIM

Date: 17.04.2025

Liberty Publishing House
Water Street Corridor New York, NY 10038
www.libertyacademicbooks.com
+1 (314) 597-0372

ISBN: 979-8-89695-056-1

CONGRESS ID

CONGRESS TITLE

CUKUROVA 14th INTERNATIONAL SCIENTIFIC RESEARCHES CONGRESS

DATE AND PLACE

March 24-26, 2025 Adana,TURKIYE

ORGANIZATION

Economic Development and Social Research Institute

ORGANIZING COMMITTEE

Prof. Dr. Salih ÖZTÜRK
Congress Chairman

Prof. Dr. Hakkı ÇİFTÇİ
Prof. Dr. İlke TAŞÇIOĞLU
Prof. Dr. Başak KARAKOÇ ÖZTÜRK
Assoc. Prof. Dr. Cavit POLAT
Assoc. Prof. Dr. Osman Cenk KANCA
Dr. Kübra İRDAY

Dr. E. İlhan ŞAHİN
Dr. Baurcan BOTAKARAYEV
Dr. M. Cenk BELİBAĞLI
Dr. Can MAVRUK
Samira KHADHRAOUI
Merve KIDIRYUZ

PARTICIPANTS COUNTRY (21 countries)

Türkiye, Albania, Nigeria, Hungary, Iraq, Pakistan, India, Uzbekistan, Algeria, Angola, Ukraine, Bangladesh, Malaysia, Morocco, Botswana, Saudi Arabia, Fiji, Serbia, Indonesia, China, Georgia

Total Accepted Article: 87
Total Rejected Papers: 17

Accepted Article (Turkey): 40

Accepted Article (Other Countries): 47

SCIENTIFIC COMMITTEE

SCIENTIFIC COMMITTEE

Dr. Osman Kubilay GÜL
Cumhuriyet University

Dr. Sarash KONYRBAEVA
Al Farabi University

Dr. Shaukat Aref Mohammed
Zakho University

Dr. Zongxian FENG
Xi`an Jiatong University

Dr. Gulizar IBRAHIMOVA
Baku Eurasia University

Dr. Sehrane KASIMI
Azerbaijan National Academy of Sciences

Dr. Akbar VALADBIGI
Urumiya University

Dr. Elvan CAFAROV
Nakhchivan University

Dr. Kazi Md. Salim Newaz
University of Malaya

Dr. Elżbieta PATKOWSKA
Lublin University of Life Sciences

Dr. Mehdi GHEISARI
Harbin Institute of Technology

Dr. Raul Duarte Salgueiral Gomes Campilho
Porto Engineering Institute

Dr. Bin ZHU
Xian Jiaotong University

Dr. Seema S. DESAI
Shivaji University

Dr. Sema KAPLAN
Erciyes University

Dr. Sonsuz KOÇYİĞİT
Batman University

Dr. Osman Cenk KANCA
Atatürk University

CUKUROVA
14th INTERNATIONAL SCIENTIFIC RESEARCHES CONFERENCE

March 24-26, 2025 / Adana, Türkiye

CONFERENCE PROGRAM

Meeting ID: 858 1117 0419

Passcode: 141414

https://us02web.zoom.us/j/85811170419?pwd=qc39oaRPJyE2i046Zr8vcotza08aGi.1

Participant Countries (21): Türkiye, Albania, Nigeria, Hungary, Iraq, Pakistan, India, Uzbekistan, Algeria, Angola, Ukraine, Bangladesh, Malaysia, Morocco, Botswana, Saudi Arabia, Fiji, Serbia, Indonesia, China, Georgia